Syntheses and Molecular and Electronic Structures of Tris(arylimido)technetium(VI) and -(V) Complexes Derived from Successive One-Electron Reductions of Tris(arylimido)iodotechnetium(VII)

Anthony K. Burrell,[1a] David L. Clark,*[,1a] Pamela L. Gordon,[1a] Alfred P. Sattelberger,[1b] and Jeffrey C. Bryan*[,1a]

Contribution from Los Alamos National Laboratory, Los Alamos, New Mexico 87545

Received September 22, 1993®

Abstract: Reduction of $Tc(NAr')_3I$ (Ar' = 2,6-dimethylphenyl) by 1 equiv of sodium generates the edge-bridged tetrahedral dimer complex $Tc_2(NAr')_4(\mu\text{-}NAr')_2$. In contrast, reduction of the more sterically hindered $Tc(NAr)_3I$ (Ar = 2,6-diisopropylphenyl) by 1 equiv of elemental sodium yields the "ethane-like" dimer $Tc_2(NAr)_6$, which can be further reduced with another equivalent of sodium (per technetium) to produce $Tc(NAr)_3^-$. $Tc(NAr)_3^-$ reacts with sources of metal cations such as $HgBr_2$ and $ClAu(PPh_3)$ to form $(ArN)_3TcHgBr$, $(ArN)_3TcHgTc(NAr)_3$, and $(ArN)_3TcAu(PPh_3)$. $Tc(NAr)_3^-$ also reacts with MeI to form $Tc(NAr)_3Me$ and with $Tc(NAr)_3I$ to form the "ethane-like" dimer $Tc_2(NAr)_6$. X-ray structural characterization of the ethane-like $Tc_2(NAr)_6$ reveals unbridged Tc–Tc and Tc–N distances of 2.744(1) and 1.758(2) Å, respectively. X-ray characterization of the tetrahedral edge-bridged $Tc_2(NAr')_6$ reveals averaged Tc–Tc, Tc–N, and Tc–μ-N distances of 2.681(2), 1.750(8), and 1.954(7) Å, respectively. X-ray analysis of $(ArN)_3TcAuPPh_3$ reveals Tc—Au, Tc═N, and Au—P distances of 2.589(1), 1,758(5), and 2.278(2) Å, respectively. Tc–Au–P, Au–Tc–N, and N–Tc–N angles are 180.0(1), 97.2(1), and 118.4(1)°. X-ray analysis of $[Tc(NAr)_3]_2Hg$ gives Tc–Hg and Tc–N distances of 2.615(1) and 1.718(10) Å and Tc–Hg–Tc, Hg–Tc–N, and N–Tc–N angles of 180.0(1), 97.6(4), and 118.3(2)°. Fenske–Hall molecular orbital calculations have been used to probe the electronic structure and bonding of tetrahedral edge-bridged and staggered ethane-like dimeric isomers of d^1–d^1 $Tc_2(NH)_6$. A "frozen π-orbital" method was utilized to separate σ- and π-bonding effects of the imido ligand to the dinuclear metal centers. Crystals of $Tc_2(NAr')_4(\mu\text{-}NAr')_2$ are monoclinic ($P2_1/n$) with a = 19.500(8) Å, b = 10.497(6) Å, c = 22.684(8) Å, β = 110.37(3)°, V = 4353 Å^3, ρ_{calc} = 1.39 g·cm^{-3}, and Z = 4. Crystals of $(ArN)_3TcHgTc(NAr)_3$ are cubic ($Pa\bar{3}$) with a = 19.560(3) Å, V = 7484 Å^3, ρ_{calc} = 1.29 g·cm^{-3}, and Z = 8. Crystals of $(ArN)_3TcAu(PPh_3)$ are rhombohedral ($R\bar{3}$) with a = 14.943(3) Å, c = 39.607(12) Å, V = 7657 Å^3, ρ_{calc} = 1.41 g·cm^{-3}, and Z = 6.

Introduction

Few complexes of technetium(VII) or -(VI) are known.[2-4] The known examples are typically oxo or oxyhalide compounds and are generally susceptible to multielectron reductions yielding lower-valent technetium products, typically in the pentavalent or lower oxidation states. Recently, imido and arylimido ligands of the general formula NR^{2-} have found an extensive use in high oxidation state transition metal inorganic and organometallic chemistry due in part to their variable steric requirements, ability to bridge more than one metal center, and variable π-bonding capabilities.[5] Our recent synthesis of high-valent $Tc(NAr)_3X$ (Ar = 2,6-diisopropylphenyl; X = alkyl, $OSiMe_3$) complexes provided new examples of relatively non-oxidizing technetium(VII) complexes.[6] Since high-valent technetium chemistry is generally dominated by multielectron reductions, we set out to explore the reduction chemistry of our new, relatively "reduction-resistant" technetium(VII) complexes to determine if one-electron reductions would be stabilized. We report here the elemental sodium reductions of $M(NAr)_3I$ and $M(NAr')_3I$ (M = Tc, Re; Ar = 2,6-diisopropylphenyl, Ar' = 2,6-dimethylphenyl) resulting in several new high-valent M(VI) and M(V) technetium and rhenium complexes, including homoleptic arylimido complexes of the general formula $M_2(NAr)_6$ and $M_2(NAr')_4(\mu\text{-}NAr')_2$ (M = Tc, Re).[7] All previous examples of structurally characterized complexes of the general formula M_2E_6, where E is a dianionic ligand such as O^{2-}, S^{2-}, Se^{2-}, or NR^{2-}, exhibit an a edge-bridged tetrahedral dimeric structure as pictured schematically below.[8-10]

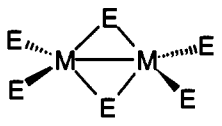

Edge-bridged tetrahedral dimer

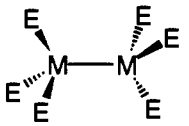

Ethanelike dimer

In contrast, M_2X_6 complexes, where X is a *mono*anionic ligand,

• Abstract published in *Advance ACS Abstracts*, April 1, 1994.

(1) (a) Inorganic and Structural Chemistry Group, CST-3, Mail Stop: C346. (b) Science and Technology Base Programs, DSTBP, Mail Stop: A116.

(2) Deutsch, E.; Libson, K.; Jurisson, S. *Prog. Inorg. Chem.* **1983**, *30*, 75–139. Clarke, M. J.; Fackler, P. H. *Struct. Bonding* **1982**, *50*, 57. Schwochau, K. *Radiochim. Acta* **1983**, *32*, 139.

(3) (a) Krebs, B. *Angew. Chem., Int. Ed. Engl.* **1969**, *8*, 381–2. (b) Herrell, A. Y.; Busey, R. H.; Gayer, K. H. *Inorg. Synth.* **1977**, *17*, 155–8. (c) Davison, A.; Jones, A. G.; Abrams, M. J. *Inorg. Chem.* **1981**, *20*, 4300–2. (d) Du Preez, J. G. H.; Gerber, T. I. A.; Gibson, M. L. *J. Coord. Chem.* **1990**, *22*, 33–42. (e) Baldas, J.; Colmanet, S. F.; Williams, G. A. *J. Chem. Soc., Dalton Trans.* **1991**, 1631–3. (f) Mercier, H. P. A.; Schrobilgen, G. J. *Inorg. Chem.* **1993**, *32*, 145–51.

(4) (a) Baldas, J.; Boas, J. F.; Bonnyman, J.; Mackay, M. F.; Williams, G. A. *Aust. J. Chem.* **1982**, *35*, 2413–22. (b) Baldas, J.; Boas, J. F.; Bonnyman, J.; Williams, G. A. *Chem. Soc., Dalto Trans.* **1984**, 2395–400. (c) Pietzsch, H. J.; Abram, U.; Kirmse, R.; Koehler, K. *Z. Chem.* **1987**, *27*, 265–6. (d) DeLearie, L. A.; Haltiwanger, R. C.; Pierpont, C. G. *J. Am. Chem. Soc.* **1989**, *111*, 4324–8. (e) Baldas, J.; Boas, J. F.; Bonnyman, J.; Colmanet, S. F.; Williams, G. A. *J. Chem. Soc., Chem. Commun.* **1990**, 1163–5. (f) Abrams, M. J.; Larsen, S. K.; Zubieta, J. *Inorg. Chem.* **1991**, *30*, 2031–5.

(5) (a) Nugent, W. A.; Haymore, B. L. *Coord. Chem. Rev.* **1980**, *31*, 123. (b) Nugent, W. A.; Mayer, J. M. *Metal-Ligand Multiple Bonds*; John Wiley and Sons: New York, 1988. (c) Wigley, D. E. *Prog. Inorg. Chem.* In press.

(6) Bryan, J. C.; Burrell, A. K.; Miller, M. M.; Smith, W. H.; Burns, C. J.; Sattelberger, A. J. *Polyhedron* **1993**, *12*, 1769–77.

(7) Portions of this work have been communicated previously: Burrell, A. K.; Bryan, J. C. *Angew. Chem.* **1993**, *105*, 85–86.

0002-7863/94/1516-3813$04.50/0

typically adopt an edge-bridged tetrahedral dimeric structure for non-bulky X, or an ethane-like structure for bulky X.[11,12] This paper reports the first ethane-like structure observed for a M_2E_6 complex, namely $Tc_2(NAr)_6$.[7] During the course of this work Schrock et al. described the reduction of $Re(NAr)_3Cl$ using a sodium amalgam. These workers report that treatment of $Re(NAr)_3Cl$ with 1 equiv of Na/Hg gives $Hg[Re(NAr)_3]_2$, while 2 equiv of Na/Hg yields $[Re(NAr)_3]^-$.[13]

Results and Discussion

Synthesis and Molecular Structures of Tc(VI) and Re(VI) Arylimido Complexes. Reaction of 1 equiv of elemental sodium with $M(NAr')_3I$ (M = Tc, Re; Ar' = 2,6-dimethylphenyl) in tetrahydrofuran gives $M_2(NAr')_4(\mu\text{-}NAr')_2$ (eq 1).[14]

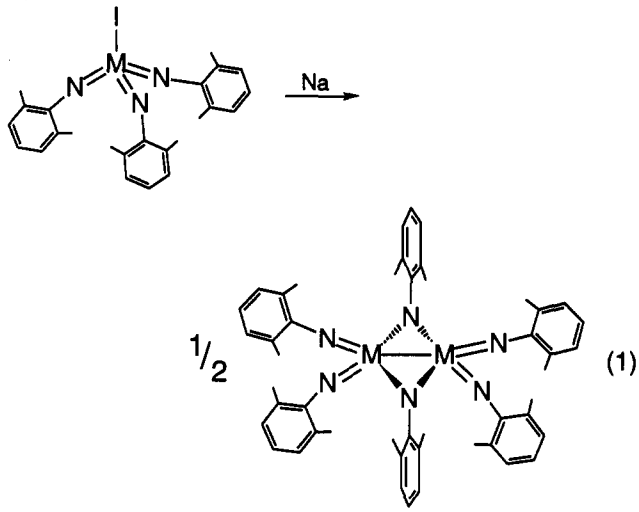

Elemental analysis of the product is consistent with an empirical formula of $Tc(NAr')_3$. The ^1H NMR spectra show two sets of resonances, in a 2:1 ratio, consistent with four terminal and two bridging arylimido ligands in an edge-bridged dimeric $Tc_2(NAr')_4(\mu\text{-}NAr')_2$ structure. This result was anticipated since the closely related rhenium complex, $Re_2(NBu^t)_4(\mu\text{-}NBu^t)_2$, adopts an edge-bridged tetrahedral dimeric structure.[8] However, exchange of bridging and terminal imido ligands is quite facile as judged by ^1H NMR spectroscopy, since the two arylimido ^1H resonances coalesce slightly above room temperature.

The edge-bridged tetrahedral dimeric configuration for $Tc_2(NAr')_4(\mu\text{-}NAr')_2$ was confirmed by X-ray structural analysis of a single crystal grown by slow evaporation of a benzene:$(Me_3Si)_2O$ solution. A summary of data collection and crystallographic parameters is given in Table 1. An ORTEP drawing showing the two independent molecules in the unit cell is shown in Figure 1. Selected bond distances and bond angles are given in the caption of Figure 1. Two separate halves of $Tc_2(NAr')_4(\mu\text{-}NAr')_2$ molecules make up the asymmetric unit, giving rise to two

Table 1. Summary of X-ray Diffraction Data

complex	$Tc_2(NAr')_6$	$(ArN)_3TcAuPPh_3$	$[Tc(NAr)_3]_2Hg$
formula	$C_{48}H_{54}N_6Tc_2$	$C_{54}H_{66}AuN_3TcP$	$C_{72}H_{102}HgN_6Tc_2$
fw	912.8	1084.0	1450.1
space group	$P2_1/n$ (No.14)	$R\bar{3}$ (No. 148)	$Pa\bar{3}$ (No. 205)
a, Å	19.500(8)	14.943(3)	19.560(3)
b, Å	10.497(6)		
c, Å	22.684(8)	39.607(12)	
β, deg	110.37(3)		
V, Å^3	4353	7657	7484
Z	4	6	8
T, °C	−70	−70	23
λ	0.71073	0.71073	0.71073
ρ_{calcd}, g·cm^{-3}	1.39	1.41	1.28
μ, cm^{-1}	6.75	32.09	24.40
scan type	θ–2θ	ω	θ–2θ
R	0.041	0.032	0.051
R_w	0.048	0.035	0.047

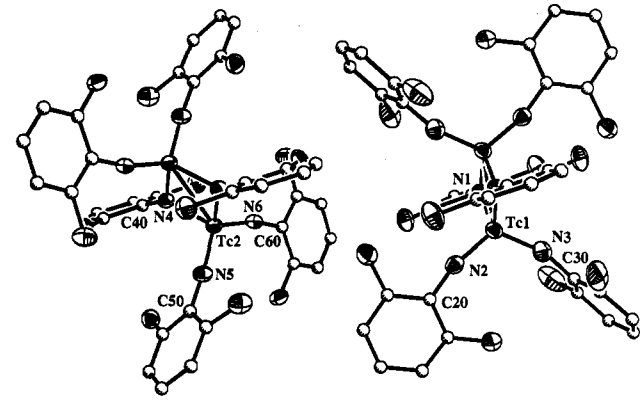

Figure 1. ORTEP (50% probability ellipsoids) drawing of $Tc_2(NAr')_4(\mu\text{-}NAr')_2$. Isotropically refined atoms are represented as shaded spheres. Selected bond lengths (Å) and angles (deg) are as follows: Tc(1)—Tc(1a) = 2.696(2), Tc(1)=N(1), 1.955(7), Tc(1)=N(2), 1.756(8), Tc(1)—N(3), 1.737(6), N(1)—Tc(1)—N(2) = 112.1(3), N(1)—Tc(1)—N(3) = 111.6(3), N(2)—Tc(1)—N(3) = 115.1(3), N(2)—Tc(1)—Tc(1a) = 123.3(2), N(3)—Tc(1)—Tc(1a) = 121.7(3), Tc(2)—Tc(2a) = 2.667(2), Tc(2)=N(4) = 1.952(6), Tc(2)=N(5) = 1.748(6), Tc(2)=N(6) = 1.759(6), N(4)—Tc(2)—N(5) = 110.9(3), N(4)—Tc(2)—N(6) = 111.6(3), N(5)—Tc(2)—N(6) = 116.4(3), N(5)—Tc(2)—Tc(2a) = 121.3(2), N(6)—Tc(2)—Tc(2a) = 122.3(2).

centrosymmetric dimers each containing a crystallographic inversion center located at the midpoint of the metal–metal bond. If the imido ligands in $Tc_2(NAr')_4(\mu\text{-}NAr')_2$ are counted as dianionic,[5] the ditechnetium core can be formally considered to contain a Tc_2^{12+} unit, giving rise to a d^1–d^1 dimer and a metal–metal single bond. The average Tc–Tc bond length of 2.68 Å is consistent with this formulation and accounts for the observed diamagnetic nature. The Tc–Tc bond lengths of 2.696(2) and 2.667(2) Å for the two independent molecules in the unit cell are well within the range of 2.54–2.73 Å exhibited by other ligand-bridged d^1–d^1 technetium dimers.[15] The bridging arylimido ligands are symmetrically displaced between the technetium metal centers, and the bridging nitrogen atoms are trigonal with the sum of the angles about N1 and N4 being 360°. The presence of high-valent Tc metal centers and planar nitrogen atoms is suggestive of some degree of Tc–N π-bonding. The distances between the technetium and bridging nitrogen atoms (1.938(6)–1.955(7) Å) are well within the range (1.88–2.14 Å) typically observed for amido technetium complexes, which are known to form Tc–N π bonds.[16]

(8) Danopoulos, A. A.; Longley, C. J.; Wilkinson, G.; Hussain, B.; Hursthouse, M. B. *Polyhedron* **1989**, *8*, 2657–2670.
(9) Danopoulos, A. A.; Wilkinson, G.; Hussain-Bates, B.; Hursthouse, M. B. *J. Chem. Soc., Dalton Trans.* **1991**, 269–275, 1855–1860.
(10) (a) Lu, Y.-j.; Ansari, M. A.; Ibers, J. A. *Inorg. Chem.* **1989**, *28*, 4049–4050. (b) Hadjikyriacou, A. I.; Coucouvanis, D. *Inorg. Chem.* **1987**, *26*, 2400–2408. (c) "MO_3" (M = Re etc.) forms polymeric structures lacking any metal–metal interaction, see: Cotton, F. A.; Wilkinson, G. *Advanced Inorganic Chemistry*, 5th ed.; John Wiley and Sons: New York, 1988.
(11) Chisholm, M. H.; Corning, J. F.; Folting, K.; Huffman, J. C. *Polyhedron* **1985**, *4*, 383–390.
(12) Summerville, R. H.; Hoffmann, R. *J. Am. Chem. Soc.* **1976**, *98*, 7240–7254.
(13) (a) Williams, D. S.; Schrock, R. R. *Organometallics* **1993**, *12*, 1148–1160. (b) Williams, D. S.; Anhaus, J. T.; Schofield, M. H.; Schrock, R. R.; Davis, W. M. *J. Am. Chem. Soc.* **1991**, *113*, 5480–5481.
(14) $Re_2(NAr')_4(\mu\text{-}NAr')_2$ has been previously mentioned.[13a]

(15) (a) Baldas, J.; Boas, J. F.; Bonnyman, J.; Colmanet, S. F.; Williams, G. A. *J. Chem. Soc., Chem. Commun.* **1990**, 1163–1165. (b) Herrmann, W. A.; Alberto, R.; Kiprof, P.; Baumgärtner, F. *Angew. Chem.* **1990**, *102*, 208; *Angew. Chem., Int. Ed. Engl.* **1990**, *29*, 189–191. (c) $Tc_2(NAr')_4(\mu\text{-}NAr')(CH_3)_2$ (Ar' = 2,6-dimethylphenyl): Burrell, A. K.; Clark, D. L.; Gordon, P. L.; Bryan, J. C. Manuscript in preparation. (d) Burrell, A. K.; Bryan, J. C. *Organometallics* **1993**, *12*, 2426–2428.

Scheme 1

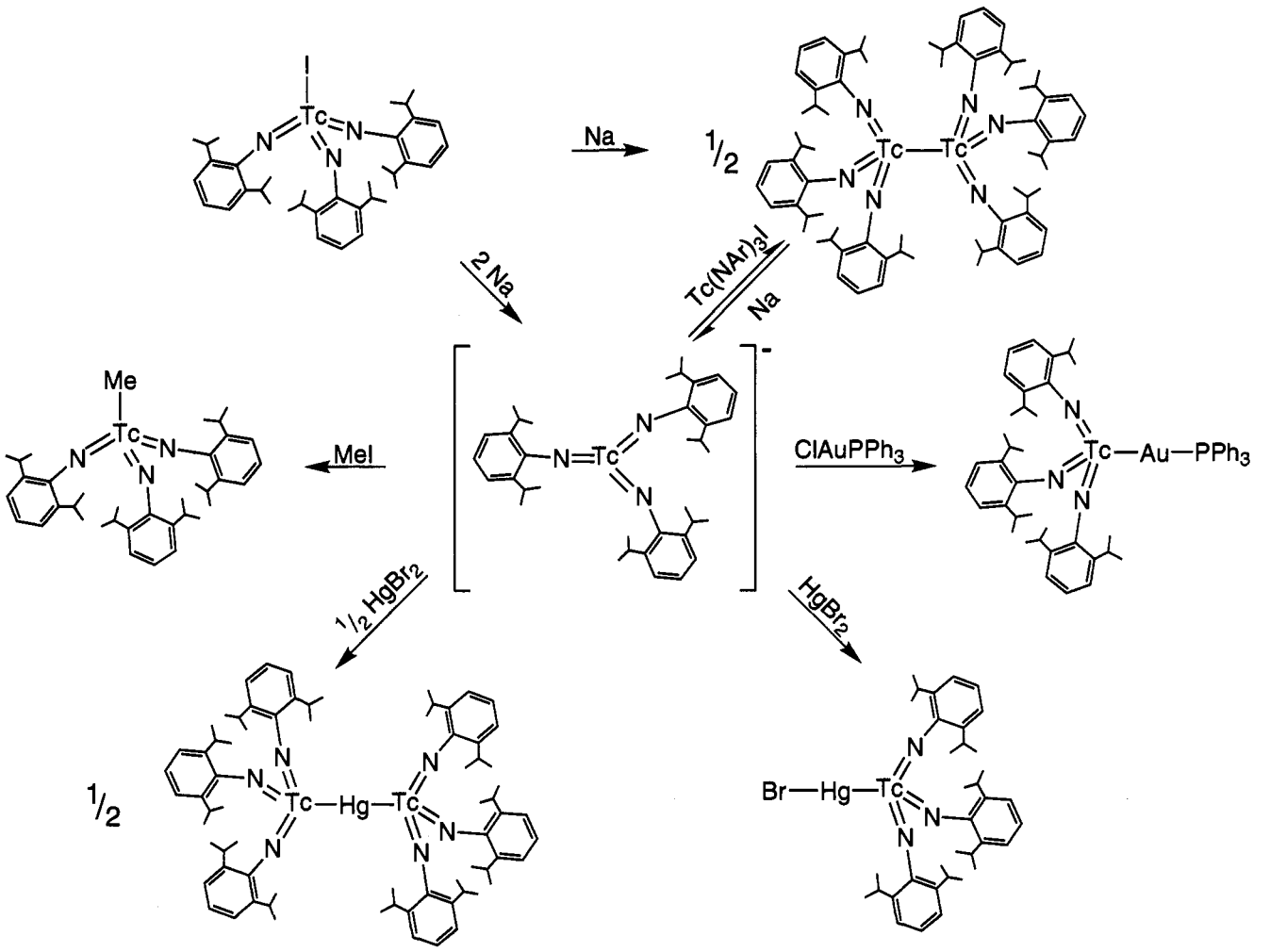

Use of the sterically more demanding 2,6-diisopropylphenylimido (NAr) ligand provides similar reaction chemistry, but reveals somewhat different spectroscopic properties (Scheme 1). A tetrahydrofuran solution of $Tc(NAr)_3I$ was treated with 1 equiv of elemental sodium, which slowly dissolved with no apparent color change. However, it was apparent that a chemical reaction had occurred since the product had different solubility characteristics from the $Tc(NAr)_3I$ starting material and appeared significantly more stable toward exposure to air. Elemental analysis of the product was again consistent with an empirical formula of $Tc(NAr)_3$. Surprisingly, the ^1H NMR spectra of the product revealed only a single arylimido ligand environment which is not consistent with an edge-bridged dimeric structure. This result is suggestive that the bulky 2,6-diisopropylphenylimido (NAr) ligand favors an alternative structure such as the ethane-like dimer. The rhenium analog, $Re_2(NAr)_6$, was obtained from a similar reaction involving sodium and $Re(NAr)_3I$ (Scheme 2).

X-ray structural analysis of a single crystal of $Tc_2(NAr)_6$, grown by slow evaporation of a THF:$(Me_3Si)_2O$ solution, revealed a Tc(VI) dimer with a staggered ethane-like geometry.[7] An ORTEP drawing is shown in Figure 2. Selected bond distances and bond angles are given in the caption of Figure 2. The two technetium metal centers are joined by an unbridged metal–metal bond and all six imido ligands are terminally bound, three to each technetium. The Tc–Tc bond lies on a crystallographic S_6 axis making all six imido ligands symmetry equivalent. As with the edge-bridged tetrahedral dimer $Tc_2(NAr')_4(\mu\text{-}NAr')_2$, the $Tc_2(NAr)_6$ complex can be formally considered to contain a Tc_2^{12+} unit, giving rise to a d^1–d^1 dimer, and a metal–metal single bond consistent with the Tc–Tc distance of 2.744(1) Å. This unbridged Tc–Tc bond is longer than that observed in $Tc_2(NAr')_4(\mu\text{-}NAr')_2$ and all other known single bond lengths for Tc^{VI}–Tc^{VI} dimers.[15] This observation may be due to steric congestion between the imido groups around the ethane-like structure or to the technetium atoms being bridged in all previous examples.

These results suggest that steric requirements may determine if d^1–d^1 M_2E_6 complexes will adopt an edge-bridged tetrahedral or ethane-like dimeric structure. Similar steric constraints imposed by the bulky 2,6-diisopropylphenylimido ligand have been observed in related imido complexes. For example, $Os(NAr)_3$ is a monomeric species,[17] whereas the less sterically demanding *tert*-butylimido analog exists as a dimer.[18] This is not to say that the 2,6-diisopropylphenylimido ligand is incapable of bridging. There are at least two examples of complexes containing a bridging 2,6-diisopropylphenylimido ligand.[19,20]

Electronic Structure and Bonding of the Tc(VI) Complexes. We sought to gain a more detailed understanding of the electronic structure and bonding in $Tc_2(NAr)_6$ complexes through use of the nonempirical, approximate molecular orbital method of Fenske and Hall.[21] We examined the electronic structure of the model compound $Tc_2(NH)_6$ idealized to D_{3d} and D_{2h} point symmetries

(16) Cambridge Crystallographic Data Base Version 5.04, October 1992. Liu, S.; Rettig, S. J.; Orvig, C. *Inorg. Chem.* **1991**, *30*, 4915–4919.

(17) Anhaus, J. T.; Kee, T. P.; Schofield, M. H.; Schrock, R. R. *J. Am. Chem. Soc.* **1990**, *112*, 1642–1643.

(18) Danopoulos, A. A.; Wilkinson, G.; Hussain-Bates, B.; Hursthouse, M. B. *J. Chem. Soc., Dalton Trans.* **1991**, 269–75.

(19) Arney, D. J.; Bruck, M. A.; Huber, S. R.; Wigley, D. E. *Inorg. Chem.* **1992**, *31*, 3749–3755.

(20) Kee, T. P.; Park, L. Y.; Robbins, J.; Schrock, R. R. *J. Chem. Soc., Chem. Commun.* **1992**, 121.

(21) Hall, M. B.; Fenske, R. F. *Inorg. Chem.* **1972**, *11*, 768.

Scheme 2

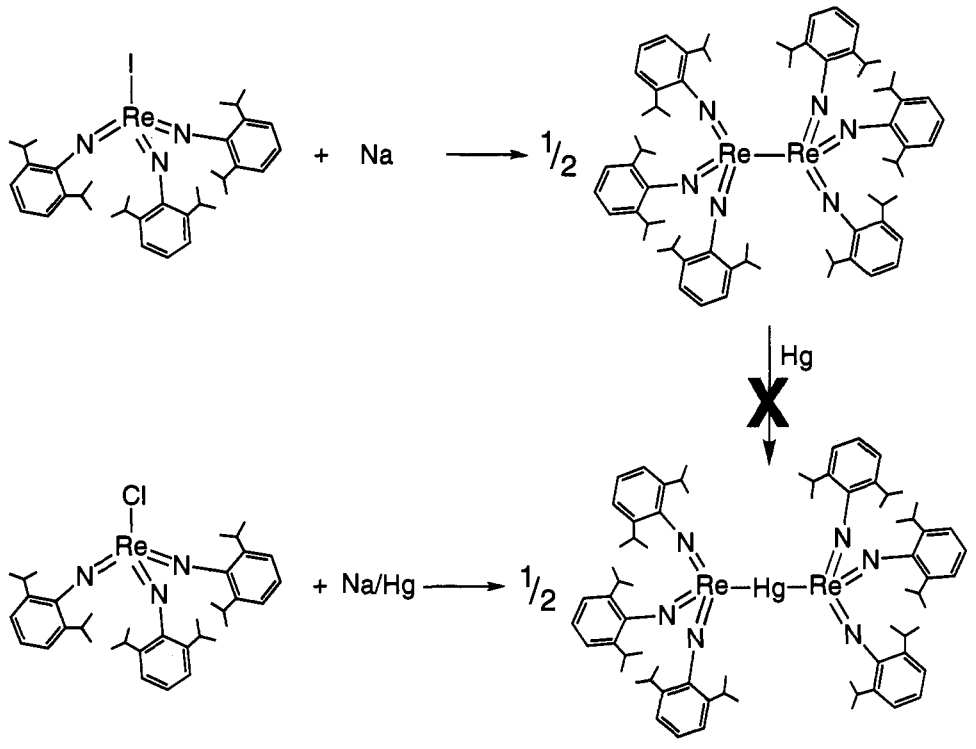

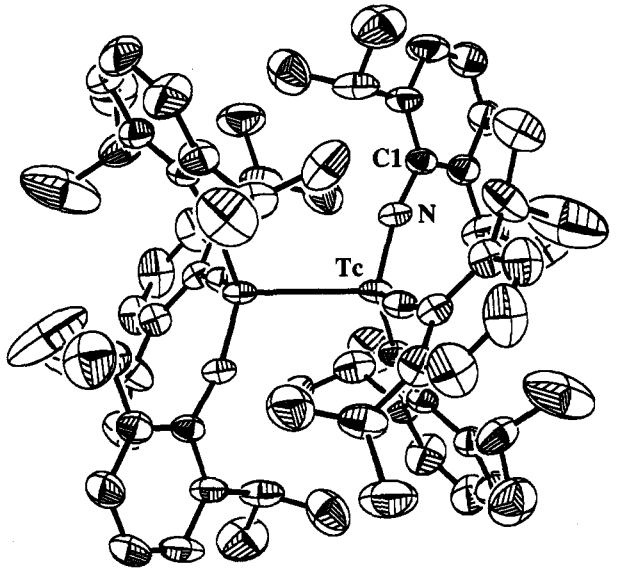

Figure 2. ORTEP (50% probability ellipsoids) drawing of $Tc_2(NAr)_6$. Selected bond lengths (Å) and angles (deg) are as follows: Tc—Tc = 2.744(1), Tc═N = 1.758(2), Tc—N—Cl = 167.6(1), N—Tc—Tc = 103.6(1), N—Tc—N = 114.6(1).[7]

(linear Tc–N–H angles) using averaged metrical parameters taken from the crystal structures of $Tc_2(NAr)_6$ and $Tc_2(NAr')_4(\mu\text{-}NAr')_2$ Both the staggered ethane-like and tetrahedral edge-bridged structure types for M_2L_6 complexes are well-known and the basic features of the electronic structure of the σ-bonding framework have been described previously.[22] However, the variable π-electron donating ability of the arylimido ligand in $Tc_2(NAr)_6$ compounds may play an important role in stabilizing one structure type over another in homoleptic complexes. Therefore it is of interest to examine the electronic structure of these two structure types supported by strong π-donating imido ligands.

A simple means of understanding the nature of M–M and M–L bonding in these two structure types is to describe the bonding interactions in terms of a $(NH)_6^{12-}$ ligand set with a common Tc_2^{12+} core. The molecular orbitals of the M_2^{n+} core are well-known and can be described according to their axial σ, π, and δ symmetry.[23] In this way we have a common basis with which to compare imido ligand interactions in the different geometries. The interaction of the NH^{2-} ligand with the Tc_2^{12+} core is readily visualized in terms of spatially and energetically inequivalent lone-pair orbitals of the free NH^{2-} ligand, derived from a sp-hybridized nitrogen atom. There is a relatively low-lying σ lone-pair and a higher-lying set of degenerate π lone-pairs depicted qualitatively in **I**.

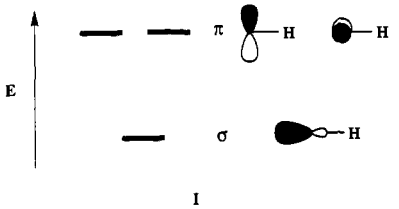

I

Ethane-like D_{3d} $Tc_2(NH)_6$. We can separate the effects of σ and π bonding by using a "frozen π orbital" computational procedure wherein the ligand π orbitals are held "frozen" so that they cannot interact with the metal center.[24] Then we observe the perturbations imposed on the electronic structure through introduction of the π bonds. In the D_{3d} point group, the set of $(NH)_6^{12-}$ σ lone-pairs span $a_{1g} + a_{2u} + e_g + e_u$ symmetry and can interact with metal-based orbitals of the Tc_2^{12+} core of the same symmetry types. This strong Tc–N σ bonding results in a stabilization of $(NH)_6^{12-}$ σ lone-pair orbitals and a concomitant

(22) (a) Bursten, B. E.; Cotton, F. A.; Green, J. C.; Seddon, E. A.; Stanley, G. C. *J. Am. Chem. Soc.* **1980**, *102*, 4579. (b) Cotton, F. A.; Stanley, G. G.; Kalbacher, B. J.; Green, J. C.; Seddon, E.; Chisholm, M. H. *Proc. Natl. Acad. Sci. U.S.A.* **1977**, *74*, 3109. (c) Hillier, I. H.; Garner, C. D.; Mitcheson, G. R. *J. Chem. Soc., Chem. Commun.* **1978**, 204. (d) Albright, T. A.; Hoffmann, R. *J. Am. Chem. Soc.* **1978**, *100*, 7736.

(23) (a) Norman, J. G., Jr.; Kolari, H. J.; Gray, H. B.; Trogler, W. C. *Inorg. Chem.* **1977**, *16*, 987. (b) Bursten, B. E.; Cotton, F. A. *Symp. Faraday Soc.* **1980**, *14*, 180.

(24) See Experimental Section and the following: Cayton, R. H.; Chisholm, M. H.; Clark, D. L.; Hammond, C. E. *J. Am. Chem. Soc.* **1989**, *111*, 2751.

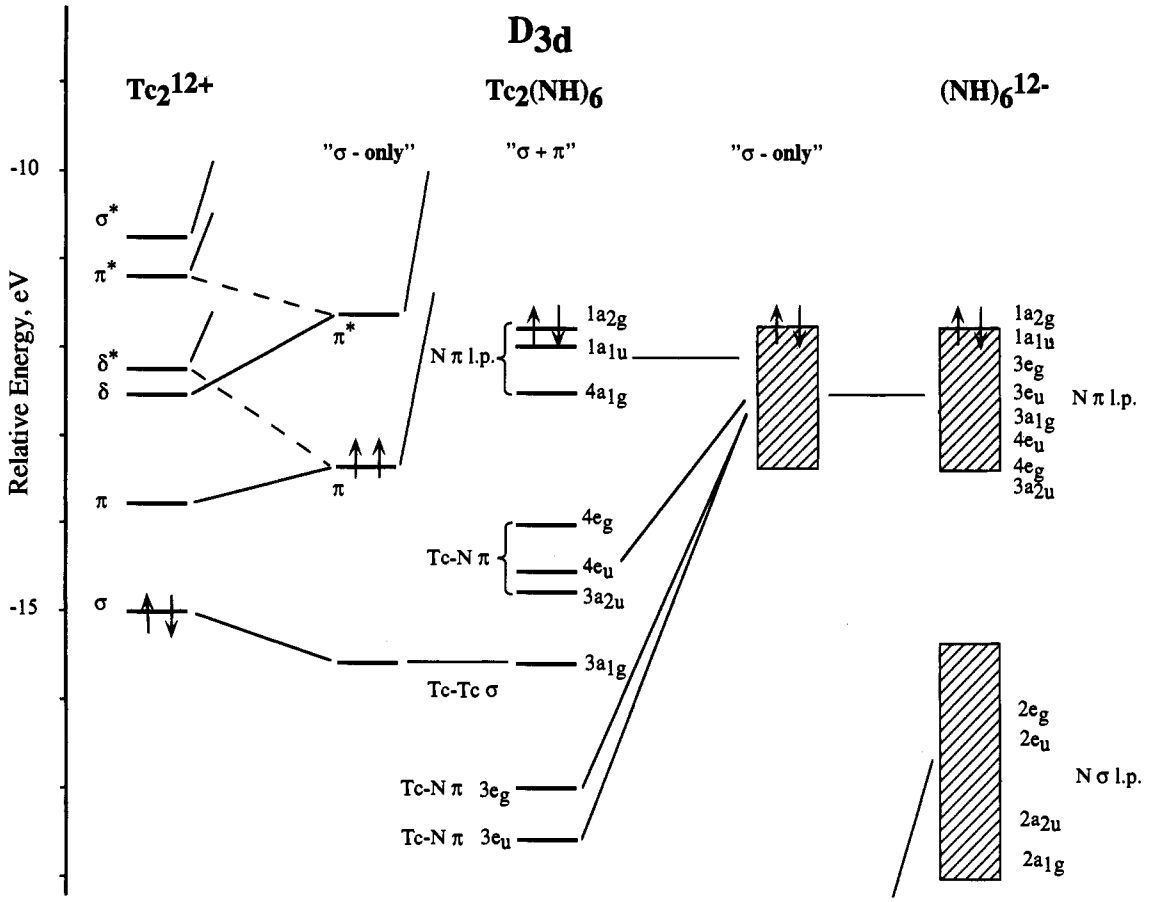

Figure 3. Molecular orbital diagram for $Tc_2(NAr)_6$ in a D_{3d} ethane-like geometry. The diagram shows the effects of metal–nitrogen σ-bonding in the columns labeled "σ-only". Metal–nitrogen π bonding effects are then added and the overall result is depicted in the column labeled "$\sigma + \pi$".

destabilization of metal-based orbitals of the same symmetry as seen in Figure 3. This "σ-only" interaction reminds us that the presence of a C_3 axis forces a mixing of Tc_2^{12+} core orbitals of π and δ symmetry. The molecular orbitals that result from this mixing contain a single nodal plane and are therefore classified as molecular orbitals of π symmetry. The resulting order of σ, π, and π^* metal-based orbitals resulting from the "σ-only" interaction is reminiscent of the ordering observed in d^3–d^3 Mo_2L_6 complexes with a $\sigma^2\pi^4$ ground state electronic structure.[22]

Next we can switch on the ligand π interactions and rationalize the effects on orbital energetics from perturbation theory. The perturbations imposed by the ligand π interactions are denoted "$\sigma + \pi$" in Figure 3 and demonstrate the relative magnitude of destabilization of metal-based orbitals as a result of strong M–L π bonding. The set of 12 π lone-pair orbitals of $(NH)_6^{12-}$ span $a_{1g} + a_{2g} + a_{1u} + a_{2u} + 2e_g + 2e_u$ symmetry in the D_{3d} point group. Lone-pair a_{2g} and a_{1u} representations do not have the appropriate symmetry to interact with any metal-based orbitals. Therefore, these orbitals come across unperturbed by the metal d orbitals and represent pure nitrogen π lone-pair orbitals in the ethane-like structure. The remaining nitrogen π lone-pairs of $a_{1g} + a_{2u} + 2e_g + 2e_u$ symmetry have the appropriate symmetry to interact with all of the remaining Tc_2^{12+} core orbitals. The metal-based σ, π, and π^* (a_{1g}, e_u, and e_g) orbitals are the only metal-based orbitals not destabilized by Tc–N σ bonding. While the a_{1g} ligand π lone-pair has the proper symmetry to interact with the Tc–Tc σ bond, these orbitals are energetically removed, have poor overlap, and represent a filled–filled interaction. Thus no net π bonding can result. In contrast, the metal-based π and π^* orbitals are energetically close and have good overlap with the ligand π lone-pair orbitals of the same symmetry. This interaction results in the formation of relatively strong, covalent Tc–N π bonds ($3e_g$ and $3e_u$ in Figure 3) at low energy and removes the Tc–Tc π and π^* orbitals from the M–M bonding manifold, resulting in a stable σ^2 electronic ground state configuration for the ethane-like structure. The e_u combination of the M–L π bonding is illustrated qualitatively in **II**.

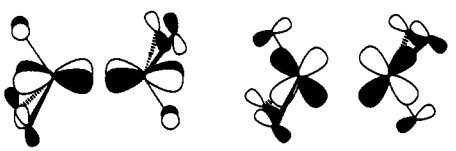

II

Edge-Bridged D_{2h} $Tc_2(NH)_6$. Under D_{2h} symmetry, the set of six $(NH)_6^{12-}$ σ lone-pair orbitals span $2a_g + b_{1g} + b_{1u} + b_{2u} + b_{3u}$ symmetry and can interact with Tc_2^{12+} core orbitals of σ and π symmetry. The interaction of ligand σ lone-pair orbitals with Tc_2^{12+} core orbitals results in a destabilization of all of the core orbitals except for the degenerate sets of δ and δ^* orbitals of the Tc_2^{12+} fragment. This "σ-only" interaction is shown in the correlation diagram of D_{2h} $Tc_2(NH)_6$ in Figure 4. From the set of 12 ligand π lone-pair orbitals, two of these ($b_{3u} + b_{2g}$) are needed to form metal–ligand σ bonds in the Tc–N–Tc bridge. These orbitals have the same symmetry as the π^* and δ^* orbitals, respectively, and their interaction results in the formation of metal–ligand σ bonds in the bridge. This bridging σ interaction can be seen as a large stabilization of b_{2g} and b_{3u} ligand π lone-pair orbitals in the "σ-only" interaction seen in Figure 4. The remaining set of Tc_2^{12+} δ-type orbitals span $a_u + b_{3g}$ symmetry in the D_{2h} point group, find no symmetry match among ligand σ lone-pairs, and come across unperturbed by the "σ-only" interaction (Figure 4). These M–L σ-bonding interactions found in $Tc_2(NH)_6$ are essentially identical to those described by Summerville and Hoffmann in their seminal studies of tetrahedral edge-bridged M_2L_6 complexes and will not be discussed further.[25]

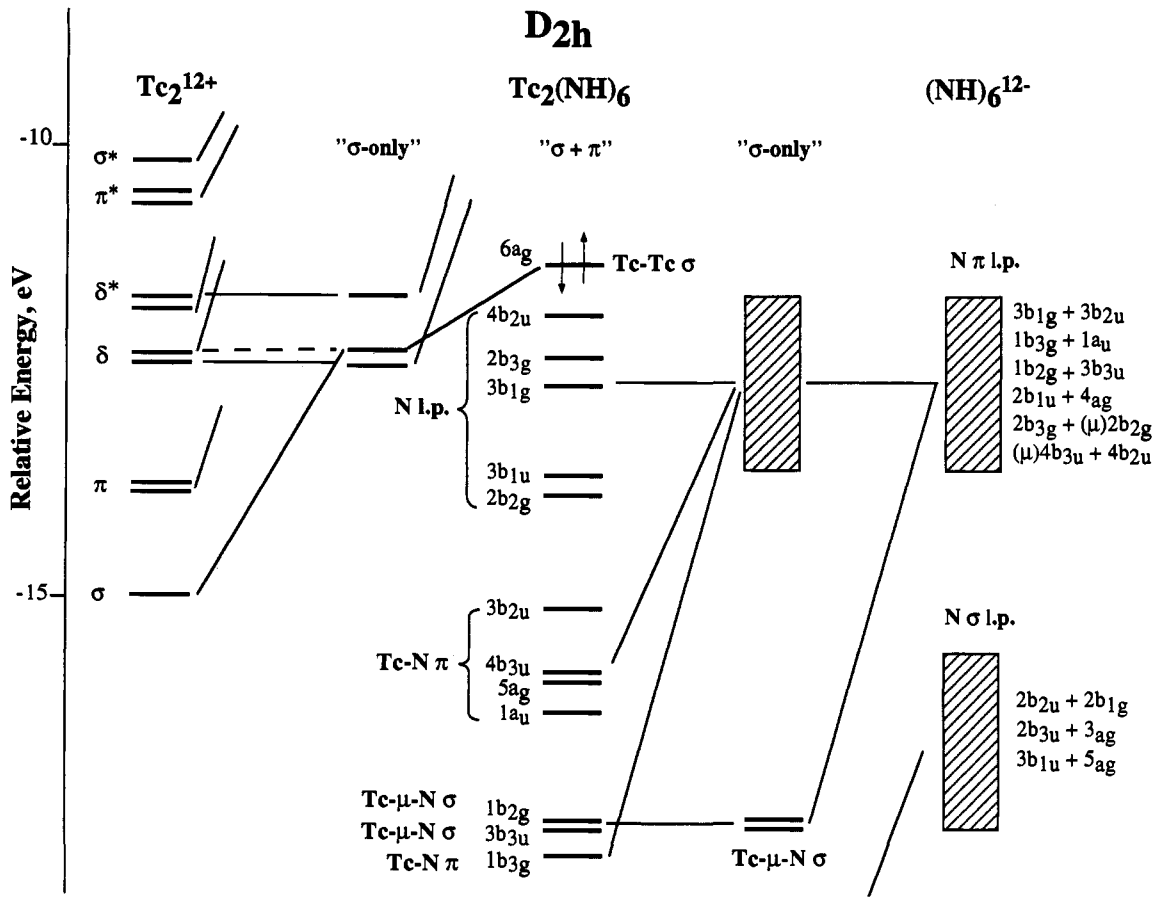

Figure 4. Molecular orbital diagram for $Tc_2(NAr')_4(\mu\text{-}NAr')_2$ in a tetrahedral edge-bridged D_{2h} geometry. The diagram shows the effects of metal–nitrogen σ-bonding in the columns labeled "σ-only". Metal–nitrogen p bonding effects are then added and the overall result is depicted in the column labeled "$\sigma + \pi$".

Next we can "switch on" the π lone-pair interactions and interpret the effects on orbital energetics from perturbation theory. The remaining set of 10 π lone-pair orbitals of $(NH)_6^{12-}$ span $a_g + b_{1g} + b_{2g} + 2b_{3g} + a_u + b_{1u} + 2b_{2u} + b_{3u}$ symmetry and find symmetry matches from nearly all of the orbitals in the M–M bonding manifold, and interaction could, in principal, result in the formation of further M–L π bonds. In practice, however, many of the M–M bonding orbitals have been pushed up high in energy as a result of strong M–L σ bonding just described. Thus while these π lone-pairs have the appropriate symmetry, many are energetically removed and thus come across as nearly pure π lone-pairs, as seen in the column labeled "$\sigma + \pi$" in Figure 4. Strong π-bonding interactions are found between ligand π lone-pairs and the b_{3g} and a_u δ-type orbitals that were unperturbed by M–L σ bonding. These interactions result in the formation of strong, covalent π bonds and are illustrated schematically in **III**. Thus for the edge-bridged dimer, the combination of ligand σ- and π-bonding interactions removes the π, δ, δ^*, and π^* M_2 core orbitals from the valence region and also yields a simple diamagnetic σ^2 ground-state electronic configuration.

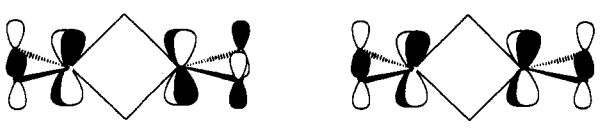

III

The Fenske–Hall calculations on the staggered ethane-like and tetrahedral edge-bridged $Tc_2(NH)_6$ dimers show clearly that both structure types are predicted to be stable when supported by the strong π-donor imido ligands. In each case, strong M–L π-bonding interactions remove the π, δ, δ^*, and π^* M_2 core orbitals from the valence region, generate a sizable HOMO–LUMO gap, and yield a simple diamagnetic σ^2 ground-state electronic configuration.

While the Fenske–Hall method is not capable of calculating a total energy difference between structure types, the discussion presented here is consistent with the edge-bridged structure being more stable due, in part, to the greater degree of metal–ligand σ bonding. Thus it would appear that the steric requirements in the bulky 2,6-diisopropylphenylimido ligand prevent bridge bond formation, giving rise to the ethane-like structure. When a smaller, less bulky arylimido ligand is used, the bridge can be formed, allowing for the more stable edge-bridged structure to predominate.

Synthesis and Molecular Structures of Tc(V) Complexes. Treatment of $Tc(NAr)_3I$ with 2 equiv of sodium or $Tc_2(NAr)_6$ with 1 equiv of sodium (per technetium) causes the green solution to rapidly change to the orange/brown color of the d^2 monomer $[Tc(NAr)_3]^-$ (Scheme 1). $[Tc(NAr)_3]^-$ may be isolated as the PPN salt (PPN = $Ph_3P{=}N{=}PPh_3^+$), prepared by the rapid addition of PPNCl to the reaction mixture. The monomeric technetium anion, in contrast to its rhenium analog, $[Re(NAr)_3]^-$,[13] is somewhat solution sensitive, decomposing slowly to an as yet unidentified mixture of compounds. Similar to $[Re(NAr)_3]^-$, reactions of $[Tc(NAr)_3]^-$ with electrophiles are quite facile.[13] When the orange/brown solution of $[Tc(NAr)_3]^-$ is added to a THF solution of Ph_3PAuCl, an immediate reaction occurs and the color of the mixture changes to green, yielding $(ArN)_3Tc\text{-}AuPPh_3$. Attempts to prepare the tris(arylimido) hydride complex "$(ArN)_3TcH$" from $[Tc(NAr)_3]^-$ and protic sources were unsuccessful. Other electrophiles were also found to react with

(25) See ref 12; also note that we have used a different coordinate system and so our orbital symmetries will not show a one-to-one correspondence.

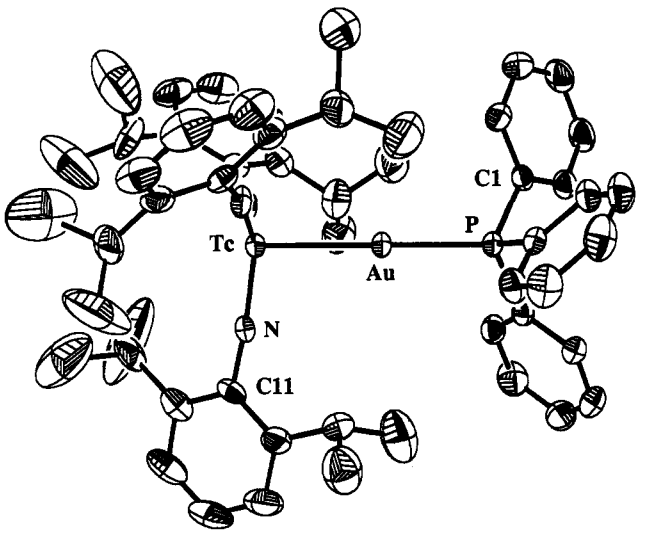

Figure 5. ORTEP (50% probability ellipsoids) drawing of $(ArN)_3TcAuPPh_3$. Selected bond lengths (Å) and angles (deg) are as follows: Tc—Au = 2.589(1), Tc=N = 1.758(5), Au—P = 2.278(2), Tc—Au—P = 180.0(1), Au—Tc—N = 97.2(1), N—Tc—N = 118.4(1).

$[Tc(NAr)_3]^-$. For example, treatment of the monomeric anion with methyl iodide gives $Tc(NAr)_3Me$,[26] and reaction with $Tc(NAr)_3I$ reforms the ethane-like dimer $Tc_2(NAr)_6$. Reaction of $[Tc(NAr)_3]^-$ with 1 equiv of $HgBr_2$ gives $(ArN)_3TcHgBr$ and 0.5 equiv of $HgBr_2$ yields $Hg[Tc(NAr)_3]_2$ as summarized in Scheme 1. Treatment of $Tc(NAr')_3I$ with 2 equiv of sodium or $Tc_2(NAr')_4(\mu\text{-}NAr')_2$ with 1 equiv of sodium (per technetium) leads to uncharacterized products.

The new Tc(V) complexes were characterized by ^1H NMR spectroscopy and elemental analysis, while the Tc(VII) methyl complex $Tc(NAr)_3Me$ was characterized by comparison with previously prepared samples.[6] Additionally, $(ArN)_3TcAuPPh_3$ and $Hg[Tc(NAr)_3]_2$ were characterized by single-crystal X-ray diffraction, since they represent the first complexes containing technetium–gold or technetium–mercury bonds.

The complex $(ArN)_3TcAuPPh_3$ (Figure 5) crystallizes in a rhombohedral space group with a long (almost 40 Å!) *c* axis. Only a portion of the molecule makes up the asymmetric unit, with the technetium, gold, and phosphorus atoms lying on a crystallographic 3-fold axis. The geometry about the technetium atom is best described as a distorted trigonal-based pyramid with gold occupying the apex. A summary of data collection and crystallographic parameters is given in Table 1. An ORTEP drawing is shown in Figure 5. Selected bond distances and bond angles are given in the caption of Figure 5. The imido ligands occupy the base, with a Au–Tc–N angle of 97.2(1)° and a N–Tc–N angle of 118.5(1)°. The Tc–Au distance of 2.589(1) Å is shorter than the Re–Au distance of 2.615(1) Å observed in $(Ph_3PAu)Re(N_2C_6H_4OMe)Cp(CO)$[27] but is indistinguishable from the Mn–Au distance of 2.573(7) Å in $(Ph_3PAu)Mn(CO)_4[P(OPh)_3]$.[28] To the best of our knowledge, these are the only other examples of structurally characterized, *terminal*, gold–phosphine complexes of the manganese triad. The relatively short Tc–Au distance observed for $(ArN)_3TcAuPPh_3$ may be a result of its higher oxidation state than the reported rhenium– and manganese–gold complexes.[29]

X-ray diffraction analysis of $Hg[Tc(NAr)_3]_2$ was performed on a single crystal grown from THF:hexane. Again, only a portion of the molecule makes up the asymmetric unit with the mercury

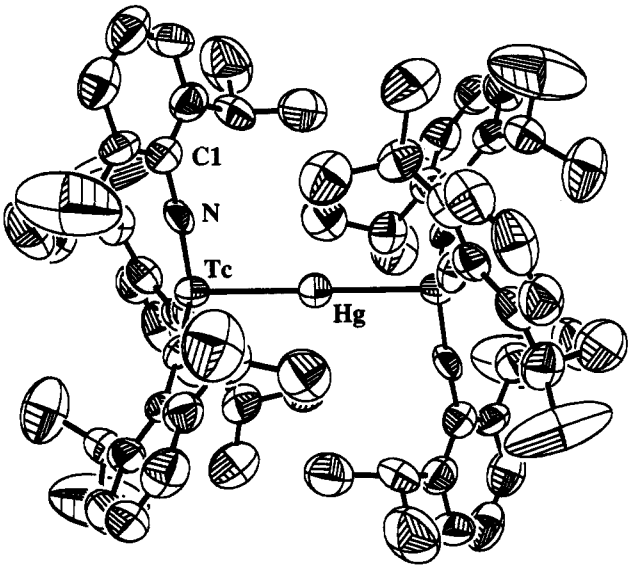

Figure 6. ORTEP (50% probability ellipsoids) drawing of $[Tc(NAr)_3]_2Hg$. Selected bond lengths (Å) and angles (deg) are as follows: Tc—Hg = 2.615(1), Tc=N = 1.718(10), Tc—Hg—Tc = 180.0(1), Hg—Tc—N = 97.6(4), N—Tc—N = 118.3(2).

and technetium atoms sitting on a crystallographic S_6 axis which relates all six imido ligands and forces them into a staggered arrangement. A summary of data collection and crystallographic parameters is given in Table 1. An ORTEP drawing is shown in Figure 6. Selected bond distances and bond angles are given in the caption of Figure 6. Like the gold complex, the geometry about technetium is best described as a distorted trigonal-based pyramid with mercury occupying the apex. Again, the imido ligands occupy the base, with a Hg–Tc–N angle of 97.6(4)° and a N–Tc–N angle of 118.3(2)°. In fact, the $Tc(NAr)_3^-$ fragments in the structures of $(ArN)_3TcAuPPh_3$ and $Hg[Tc(NAr)_3]_2$ are almost identical, suggesting that the nature of the metal cation has little effect on $Tc(NAr)_3^-$. The structure of $Hg[Tc(NAr)_3]_2$ is almost identical to its rhenium analog $Hg[Re(NAr)_3]_2$, recently reported by the Schrock group.[13] The only significant differences are the M–Hg (2.621(1) Å, Re; 2.615(1) Å, Tc) and M–N (1.76(1) Å, Re; 1.718(10) Å, Tc) distances.

Relevance to Related $Re(NAr)_3Cl$ Reductions. Williams and Schrock report that treatment of $Re(NAr)_3Cl$ with 1 equiv of Na/Hg gives $Hg[Re(NAr)_3]_2$ in roughly 50% yield, while treatment of $Re(NAr)_3Cl$ *or* $Hg[Re(NAr)_3]_2$ with 2 equiv of Na/Hg yields $[Re(NAr)_3]^-$.[13] Our work clearly demonstrates that in the absence of Hg, sodium will reduce $M^{VII}(NAr)_3I$ to $M_2^{VI}(NAr)_6$ and $M^V(NAr)_3^-$ by successive one-electron reductions. We wondered if this meant that the rhenium^{VI} dimer $Re_2(NAr)_6$ was reactive toward Hg. Both $Re_2(NAr)_6$ and $Tc_2(NAr)_6$ are unreactive toward elemental mercury, even under simple photolysis, on heating to 80 °C, or upon sonication. It is reasonable therefore to assume that, in the reactions carried out by Schrock et al., $Re^{VI}_2(NAr)_6$ is not a precursor to $Hg[Re(NAr)_3]_2$. It is therefore probable that $Re(NAr)_3Cl$ is reduced by one electron to the monomeric Re^{VI} radical $^{\bullet}Re(NAr)_3$ or radical anion $^{-\bullet}Re(NAr)_3$ which in turn are reduced by Hg to form $Hg[Re(NAr)_3]_2$. Also of particular relevance to the sodium amalgam reductions of $Re(NAr)_3Cl$, carried out by Schrock et al.,[13] are the reactions of $[Tc(NAr)_3]^-$ with $HgBr_2$. For the products of these reactions, $[Tc(NAr)_3]HgBr$ and $Hg[Tc(NAr)_3]_2$, it is reasonable to assign the formal oxidation states of the technetium and mercury as Tc(V) and Hg(II).

Concluding Remarks

The unbridged ethane-like structure of $M_2(NAr)_6$ (M = Tc, Re) represents a completely new structural type for the M_2E_6

(26) $Tc(NAr)_3Me$ can also be prepared by reacting methyl Grigard with $Tc(NAr)_3(OSiMe_3)$ or $Tc(NAr)_3I$.[6]
(27) Barrientos-Penna, C. F.; Einstein, F. W. B.; Jones, T.; Sutton, D. *Inorg. Chem.* **1985**, *24*, 632–634.
(28) Mannan, K. A. I. F. M. *Acta Crystallogr.* **1967**, *23*, 649–653.
(29) Melnik, M.; Van Lier, J. *Coord. Chem. Rev.* **1987**, *77*, 275.

systems. The factors influencing the formation of either ethane-like or the more common edge-bridged tetrahedral dimer configuration appear to be purely steric, with the edge-bridged tetrahedral dimer existing in the electronically more favorable configuration. This is most readily demonstrated by a comparison of the structures of $Tc_2(NAr)_6$ and $Tc_2(NAr')_6$, both of which contain arylimido ligands and are therefore essentially electronically identical. As with all previously reported M_2E_6 complexes $Tc_2(NAr')_6$ adopts the edge-bridged tetrahedral dimer configuration, whereas the more sterically congested $Tc_2(NAr)_6$ exists exclusively as the ethane-like structure. These two dimeric compounds represent the first examples of structurally characterized homoleptic imido complexes for technetium.

The formation of the $[Tc(NAr)_3]^-$ proceeds without difficulty and this anionic complex has proven to be a good nucleophile reacting with a number of electrophiles and resulting in the first examples of complexes containing technetium–mercury and technetium–gold bonds.

Experimental Section

General Considerations. *Caution!* The isotope ^{99}Tc used in the syntheses of all technetium complexes described in this paper is a low-energy β^- emitter (E_{max} = 0.29 MeV) with a very long half-life (2.1×10^5 years). All experiments are performed in laboratories designated and approved for low-level radioactive materials following procedures and techniques described elsewhere.[6] Toluene, benzene, hexane, THF, and hexamethyldisiloxane were distilled under N_2 from sodium or sodium/potassium alloy. Ammonium pertechnetate was obtained from Oak Ridge National Laboratory and was purified as described previously.[30] $Tc(NAr')_3I$[6] and $Tc(NAr)_3I$[7] were prepared following published procedures. $ISiMe_3$ (Aldrich) was distilled and stored in a drybox prior to use. Spectral data, elemental analyses, X-ray data collection, reduction, solution, and refinement were performed as described previously.[6]

$Tc_2(NAr)_6$: (a) Na (3 mg, 0.13 mmol) was added to a solution of $Tc(NAr)_3I$ (100 mg, 0.13 mmol) in THF (15 mL). The mixture was stirred for approximately 3 h, after which the solvent was removed from the green solution *in vacuo*. The residue was then extracted with $(Me_3Si)_2O$ (15 mL) and filtered through Celite. Evaporation of the $(Me_3Si)_2O$ gave the product as a green solid (68 mg, 79%). This solid was then purified by column chromatography with silica gel using hexane:toluene (9:1) as an eluent. ^1H NMR (C_6D_6, 295 K, ppm): δ 6.97 (m, $C_6H_3{}^iPr_2$, 9H), 3.94 (hep, $CHMe_2$, 6H, ^2J = 6.8 Hz), 1.08 (d, $CHCH_3$, 36H, ^2J = 6.8 Hz). ^{13}C NMR (62.8 MHz, CD_2Cl_2, 295 K, ppm): δ 144.3 (NC), 128.1 (Ar), 126.8 (Ar), 123.5 (Ar), 28.3 (CH), 24.0 (CH_3). Anal. Calcd for $Tc_2C_{72}H_{102}N_6$: C, 69.20; H, 8.23; N, 6.72. Found: C, 68.71; H, 8.39; N, 6.58.

(b) Na sand (6 mg, 0.26 mmol) was added to a solution of $TcI(NAr)_3$ (100 mg, 0.13 mmol) in THF (15 mL). The mixture was stirred until the green color was no longer evident. The solution was then filtered through Celite into a solution containing $TcI(NAr)_3$ (100 mg, 0.13 mmol). The resulting green solution was then stirred for 30 min. The product was isolated as above (130 mg, 75%).

$Re(NAr)_3I$: Iodotrimethylsilane (0.6 mL, 0.42 mmol) was added to a solution of $Re(OSiMe_3)(NAr)_3$ (100 mg, 0.12 mmol) in toluene (15 mL). The mixture was stirred for approximately 1 h, after which the solvent was removed *in vacuo*. The residue was then extracted with hot hexamethyldisiloxane ($(Me_3Si)_2O$, 15 mL) and filtered through Celite. The solution was cooled to –40 °C for 12 h and then filtered to give the product as a dark red solid (100 mg, 95%). ^1H NMR (C_6D_6, 295 K, ppm): δ 7.01 (m, $C_6H_3{}^iPr_2$, 9H), 3.69 (hep, $CHMe_2$, 6H, ^2J = 6.9 Hz), 1.10 (d, $CHCH_3$, 36H, ^2J = 6.9 Hz). Anal. Calcd for $ReC_{36}H_{51}N_3I$: C, 51.54; H, 6.13; N, 5.01. Found: C, 51.08; H, 6.39; N, 4.86.

$Re(NAr)_6$: Na (3 mg, 0.13 mmol) was added to a solution of $Re(NAr)_3I$ (100 mg, 0.12 mmol) in THF (15 mL). The mixture was stirred for approximately 3 h, after which the solvent was removed from the red solution *in vacuo*. The residue was then extracted with $(Me_3Si)_2O$ (15 mL) and filtered through Celite. Evaporation of the $(Me_3Si)_2O$ gave the product as a red solid (68 mg, 80%). This solid was then purified by column chromatography with silica gel using hexane:toluene (9:1) as an eluent. ^1H NMR (C_6D_6, 295 K, ppm): δ 7.01 (m, $C_6H_3{}^iPr_2$, 9H), 3.72 (hep, $CHMe_2$, 6H, ^2J = 6.9 Hz), 1.11 (d, $CHCH_3$, 36H, ^2J = 6.9 Hz). Anal. Calcd for $Re_2C_{72}H_{102}N_6$: C, 60.73; H, 7.22; N, 5.90. Found: C, 60.74; H, 7.16; N, 5.78.

$Re_2(NAr')_6$:[14] Na sand (3.5 mg, 0.15 mmol) was added to a solution of $ReI(NAr')_3$ (100 mg, 0.15 mmol) in THF (15 mL). The mixture was stirred for approximately 3 h, after which the solvent was removed from the red solution *in vacuo*. The residue was then extracted with benzene (15 mL), filtered through Celite, and purified by column chromatography on Alumina. Addition of $(Me_3Si)_2O$ and cooling the solution yields the product as a red solid (79 mg, 97%). ^1H NMR (C_6D_6, 295 K, ppm): δ 7.05 (m, $C_6H_3Me_2$, 6H), 6.70 (m, $C_6H_3Me_2$, 12H), 2.16 (s, CH_3, 12H), 2.15 (s, CH_3, 24H). Anal. Calcd for $Re_2C_{48}H_{54}N_6$: C, 53.02; H, 5.01; N, 7.73. Found: C, 53.51; H, 5.48; N, 6.79.

[PPN][$(ArN)_3Tc$]: Na sand (6 mg, 0.26 mmol) was added to a solution of $TcI(NAr)_3$ (100 mg, 0.13 mmol) in THF (15 mL). The mixture was stirred until the green color was no longer evident and the solution was deep orange. The solution was then filtered through Celite into a solution containing PPNCl (74 mg, 0.13 mmol). This new solution was then stirred for 10 min. The solvent was removed *in vacuo* and the residue extracted with benzene (20 mL). The benzene solution was filtered through Celite and the product obtained as orange crystals (62 mg, 41%) by addition of hexamethyldisiloxane ($(Me_3Si)_2O$) (30 mL). ^1H NMR (d_8-THF, 295 K, ppm): δ 7.6–6.6 (m, $C_6H_3{}^iPr_2$ and PC_5H_5, 24H), 4.17 (hep, $CHMe_2$, 6H, ^2J = 7.4 Hz), 1.09 (d, $CHCH_3$, 36H, ^2J = 7.4 Hz). Anal. Calcd for $P_2TcC_{72}H_{81}N_4$: C, 74.40; H, 7.02; N, 4.84. Found: C, 74.25; H, 7.50; N, 4.67.

$(ArN)_3TcHgTc(NAr)_3$: Na sand (6 mg, 0.26 mmol) was added to a solution of $TcI(NAr)_3$ (100 mg, 0.13 mmol) in THF (15 mL). The mixture was stirred until the green color was no longer evident. The solution was then filtered through Celite into a solution containing $HgBr_2$ (23 mg, 0.06 mmol). The resulting green solution was then stirred for 30 min. The solvent was removed *in vacuo* and the residue extracted with benzene (20 mL). The benzene solution was filtered through Celite and the product obtained as dark red/orange crystals from the addition of $(Me_3Si)_2O$ (30 mL). The complex was further purified by slow recrystalization from C_6H_6:$(Me_3Si)_2O$ and gave the product as red crystals (82 mg, 85%). ^1H NMR (C_6D_6, 295 K, ppm): δ 7.00 (m, $C_6H_3{}^iPr_2$, 9H), 4.05 (hep, $CHMe_2$, 6H, ^2J = 6.8 Hz), 1.34 (d, $CHCH_3$, 36H, ^2J = 6.8 Hz). Anal. Calcd for $HgTc_2C_{72}H_{102}N_6$: C, 59.71; H, 7.10; N, 5.80. Found: C, 60.14; H, 7.16; N, 5.78.

$(ArN)_3TcHgBr$: Na sand (6 mg, 0.26 mmol) was added to a solution of $TcI(NAr)_3$ (100 mg, 0.13 mmol) in THF (15 mL). The mixture was stirred until the green color was no longer evident. The solution was then filtered through Celite into a solution containing $HgBr_2$ (46 mg, 0.13 mmol). The resulting dark green solution was then stirred for 30 min. The solvent was removed *in vacuo* and the residue extracted with benzene (20 mL). The benzene solution was filtered through Celite and the product obtained as dark green/black crystals by the addition of $(Me_3Si)_2O$ (30 mL). The complex was further purified by slow recrystalization from C_6H_6:$(Me_3Si)_2O$ and gave the product as dark-green crystals (77 mg, 87%). ^1H NMR (C_6D_6, 295 K, ppm): δ 6.99 (m, $C_6H_3{}^iPr_2$, 9H), 3.67 (hep, $CHMe_2$, 6H, ^2J = 6.8 Hz), 1.10 (d, $CHCH_3$, 36H, ^2J = 6.8 Hz). Anal. Calcd for $HgBrTcC_{36}H_{51}N_3$: C, 47.77; H, 5.68; N, 4.65. Found: C, 47.40; H, 5.11; N, 4.26.

$(ArN)_3TcAuPPh_3$: Na sand (6 mg, 0.26 mmol) was added to a solution of $TcI(NAr)_3$ (100 mg, 0.13 mmol) in THF (15 mL). The mixture was stirred until the green color was no longer evident. The solution was then filtered through Celite into a solution containing $ClAuPPh_3$ (64 mg, 0.13 mmol). The resulting green solution was then stirred for 30 min. The solvent was removed *in vacuo* and the residue extracted with benzene (20 mL). The benzene solution was filtered through Celite and the product obtained as dark green crystals by the addition of $(Me_3Si)_2O$ (30 mL). The complex was further purified by slow recrystalization from C_6H_6:$(Me_3Si)_2O$ and gave the product as dark-green crystals (125 mg, 89%). ^1H NMR (C_6D_6, 295 K, ppm): δ 7.39 (m, PC_5H_5, 6 H), 7.10–6.91 (m, $C_6H_3{}^iPr_2$ and PC_5H_5, 18H), 4.39 (hep, $CHMe_2$, 6H, ^2J = 6.8 Hz), 1.27 (d, $CHCH_3$, 36H, ^2J = 6.8 Hz). Anal. Calcd for $AuPTcC_{54}H_{66}N_3$: C, 59.88; H, 6.14; N, 3.88. Found: C, 59.56; H, 6.73; N, 4.07.

$(ArN)_3TcCH_3$: Na sand (6 mg, 0.26 mmol) was added to a solution of $TcI(NAr)_3$ (100 mg, 0.13 mmol) in THF (15 mL). The mixture was stirred until the green color was no longer evident. The solution was then filtered through Celite into a solution containing methyl iodide (19 mg, 0.13 mmol). The resulting green solution was then stirred for 30 min. The solvent was removed *in vacuo* and the residue extracted with benzene (20 mL). The benzene solution was filtered through Celite and the product obtained as dark-green crystals by the addition of $(Me_3Si)_2O$ (30 mL). The complex was further purified by slow recrystalization from C_6H_6:

(30) Libson, K.; Barnett, B. L.; Deutsch, E. *Inorg. Chem.* **1983**, *22*, 1695–1704.

$(Me_3Si)_2O$ and gave the product as dark-green crystals (5 mg, 72%). The product was characterized by comparison to an authentic sample.[6]

$Tc_2(NAr')_6$: Na sand (4 mg, 0.17 mmol) was added to a solution of $TcI(NAr')_3$ (100 mg, 0.17 mmol) in THF (15 mL). The mixture was stirred for approximately 3 h, after which the solvent was removed from the red solution *in vacuo*. The residue was then extracted with benzene (15 mL), filtered through Celite, and purified by column chromatography on Alumina. Addition of $(Me_3Si)_2O$ and cooling the solution gave the product as a red solid (74 mg, 95%). This solid was then purified by column chromatography with silica gel using hexane:toluene (9:1) as an eluent. ^1H NMR (C_6D_6, 295 K, ppm): δ 7.05 (m, $C_6H_3Me_2$, 6H), 6.70 (m, $C_6H_3Me_2$, 12H), 2.19 (s, CH_3, 12H), 2.18 (s, CH_3, 24H). ^{13}C NMR (62.8 MHz, CD_2Cl_2, 295 K, ppm): δ 134.5, 132.3, 132.2, 128.9, 128.7, 127.9, 127.7, 126.3, 19.4, 19.1. Anal. Calcd for $Tc_2C_{48}H_{54}N_6$: C, 63.39; H, 5.97; N, 9.22. Found: C, 63.01; H, 6.14; N, 9.51.

Computational Procedures. We have employed model compounds of the formula $Tc_2(NH)_6$ to investigate the nature of Tc–N π-bonding in the two different $Tc_2(NR)_6$ geometries described in the text. For the staggered, ethane-like geometry $Tc_2(NAr)_6$, terminal Tc–Tc, Tc–N, and N–H distances were set at 2.744, 1.758, and 1.01 Å, respectively. The coordinates for $Tc_2(NAr)_6$ were idealized to perfect D_{3d} symmetry with Tc–Tc–N and Tc–N–H angles of 103.6 and 180°. The coordinates for $Tc_2(NAr')_4(\mu\text{-}NAr')_2$ were idealized to perfect D_{2h} symmetry with terminal Tc–Tc, Tc–N, and N–H distances set at 2.667, 1.748, and 1.01 Å, respectively. Bridging Tc–N bond lengths were set at 1.944 Å. Terminal Tc–Tc–N and Tc–N–H angles were 123.5 and 180°.

Molecular orbital calculations were performed by the method of Fenske and Hall, which has been described in detail elsewhere.[21] The Fenske–Hall method is an approximate Hartree–Fock–Roothaan SCF-LCAO procedure, and the final results depend only upon the chosen atomic basis set and internuclear distances.

All atomic wave functions were generated by a best fit to Herman–Skillman atomic calculations using the method of Bursten, Jensen, and Fenske.[31] Contracted double-ζ representations were used for Tc 4d and N 2p AO's while single-z functions were used for all other orbitals. Valence AO's were orthogonalized to all other valence and core orbitals on the same atom. Basis functions for the technetium atom were derived for a +1 oxidation state with the valence 5s and 5p exponents fixed at 2.0 and 1.6. An exponent of 1.16 was used for the H 1s atomic orbital.[32] SCF calculations were performed in the atomic basis on the $(NH)_6^{12-}$ and Tc_2^{12+} fragments and on the $Tc_2(NH)_6$ complexes in each geometry. Following convergence, the results were transformed into a basis of the canonical orbitals of the Tc_2^{12+} and the $(NH)_6^{12-}$ ligand sets. All calculations were converged with a self-consistent-field iterative technique by using a convergence criteria of 0.0010 as the largest deviation between atomic orbital populations for successive cycles. In the "frozen π-orbital" method, the ligand p orbitals of $(NH)_6^{12-}$ canonical basis are partitioned in the Fock and overlap matrices in a similar fashion to the partitioning of the matrices of a diatomic molecule into core and valence regions as illustrated by Roothan.[33] The orbitals were then deleted from variational treatment.[34] All calculations described in this paper were obtained using a VAX 8800 or Macintosh IIci computer system.

Acknowledgment. The authors thank M. M. Miller for assistance with the X-ray structure of $Hg[Tc(NAr)_3]_2$. We also thank D. E. Wigley and S. D. McKee for helpful discussions. This work was supported by Laboratory Directed Research and Development and performed under the auspices of the U.S. Department of Energy at Los Alamos National Laboratory.

Supplementary Material Available: Complete tabulations of bond lengths and angles, atomic coordinates, thermal parameters, and completely labeled diagrams for $Tc_2(NAr')_4(\mu\text{-}NAr')_4$, $(ArN)_3TcAuPPh_3$, and $[Tc(NAr)_3]_2Hg$ (16 pages). This material is contained in many libraries on microfiche, immediately follows this article in the microfilm version of the journal, and can be ordered from the ACS; see any current masthead page for ordering information.

(31) Bursten, B. E.; Jensen, J. R.; Fenske, R. F. *J. Chem. Phys.* **1978**, *68*, 3320.

(32) Hehre, W. J.; Stewart, R. F.; Pople, J. A. *J. Chem. Phys.* **1969**, *51*, 2657.

(33) Roothan, C. C. *J. Rev. Mod. Phys.* **1951**, *23*, 69.

(34) A discussion of the computational procedure has been published. Lichtenberger, D. L.; Fenske, R. F. *J. Chem. Phys.* **1976**, *64*, 4247.